Oxyhalogen–sulfur chemistry — Kinetics and mechanism of the bromate oxidation of cysteamine

Moshood K. Morakinyo, Edward Chikwana, and Reuben H. Simoyi

Abstract: The kinetics and mechanism of the oxidation of the biologically important molecule, cysteamine, by acidic bromate and molecular bromine have been studied. In excess acidic bromate conditions, cysteamine is oxidized to N-brominated derivatives, and in excess cysteamine the oxidation product is taurine according to the following stoichiometry: $BrO_3^- + H_2NCH_2CH_2SH \rightarrow H_2NCH_2CH_2SO_3H + Br^-$. There is quantitative formation of taurine before N-bromination commences. Excess aqueous bromine oxidizes cysteamine to give dibromotaurine: $5Br_2 + H_2NCH_2CH_2SH + 3H_2O \rightarrow Br_2NCH_2CH_2SO_3H + 8Br^- + 8H^+$, while excess cysteamine conditions gave monobromotaurine. The oxidation of cysteamine by aqueous bromine is effectively diffusion-controlled all the way to the formation of monobromotaurine. Further formation of dibromotaurine is dependent on acid concentrations, with highly acidic conditions inhibiting further reaction towards formation of dibromotaurine. The formation of the N-brominated derivatives of taurine is reversible, with taurine regenerated in the presence of a reducing agent such as iodide. This feature makes it possible for taurine to moderate hypobromous acid toxicity in the physiological environment.

Key words: cysteamine, hypobromous acid, toxicities, antioxidant.

Résumé : On a étudié la cinétique et le mécanisme de l'oxydation de la molécule biologiquement importante, cystéamine, par le bromate acide et le brome moléculaire. Dans des conditions de bromate acide en excès, la cystéamine est oxydée en dérivés bromés et, dans un excès de cystéamine, le produit d'oxydation est la taurine qui est formée en d'après la stoechiométrie: $BrO_3^- + H_2NCH_2CH_2SH \rightarrow H_2NCH_2CH_2SO_3H + Br^-$. Il y a formation quantitative de taurine avant que la N-bromation commence. Un excès de brome en milieu aqueux provoque une oxydation de la cystéamine avec formation de dibromotaurine: $5Br_2 + H_2NCH_2CH_2SH + 3H_2O \rightarrow Br_2NCH_2CH_2SO_3H + 8Br^- + 8H^+$, alors que les conditions dans lesquelles la cystéamine est en excès conduit à la formation de la monobromotaurine. L'oxydation de la cystéamine par le brome aqueux est effectivement une réaction sous contrôle de la diffusion jusqu'à la formation de la monobromotaurine. La formation subséquente de dibromotaurine dépend des concentrations d'acide alors que les conditions fortement acides inhibent la réaction subséquente pouvant conduire à la formation de la dibromotaurine. La formation des dérivés N-bromés de la taurine est réversible, la taurine pouvant être régénérée en présence d'un agent réducteur, tel un ion iodure. Cette caractéristique fait que la taurine peut réduire le caractère toxique de l'acide hypobromeux dans un environnement physiologique.

Mots-clés : cystéamine, acide hypobromeux, toxicités, antioxydant.

[Traduit par la Rédaction]

Introduction

Sulfur metabolism in biological systems is believed to be the main source of thiols (1, 2). The most important thiols in biological chemistry are cysteine, homocysteine, and glutathione. Glutathione is the most abundant non-protein thiol in mammals, an adult human having about 30 g glutathione widely distributed in most tissues, with levels in the kidney and liver significantly higher (3). In general, thiols are readily oxidized to disulfides in the presence of mild oxidants, and in the presence of more powerful oxidants S-oxygenation can occur, which yields, successively, sulfenic, sulfinic, and sulfonic acids. In some cases, the C–S bond cleaves to give sulfate as the final oxidation product (2, 4). Those thiols without an amino group adjacent to the sulfhydryl group are easily oxidized to sulfate and a mixture of alcohols, aldehydes, and carboxylic acids (depending on the amount and strength of oxidant). α-Aminothiols are very reactive, but will not easily cleave the C–S bond, and can thus be regenerated for further use after oxidation to the S-oxide or the disulfide (5). Sulfinic and sulfonic acids formed from thiols with an amino group on the α or β position have been found to be quite stable (6, 7).

In living systems, S-oxygenation of the thiol group in the physiological environment can be initiated by two microsomal systems: one involving cytochrome P-450 sys-

Received 30 August 2007. Accepted 6 February 2008. Published on the NRC Research Press Web site at canjchem.nrc.ca on 5 April 2008.

M.K. Morakinyo, E. Chikwana,[1] and R.H. Simoyi.[2] Department of Chemistry, Portland State University, Portland, OR 97207-0751, USA.

[1]Present address: Department of Chemistry & Biochemistry, California State University-Chico, CA 95929-0210, USA.
[2]Corresponding Author (e-mail: rsimoyi@pdx.edu).

 doi:10.1139/V08-031

tem of enzymes and the other based on the flavin-containing monooxygenase (8–10). In the presence of these enzyme systems and cofactor-like compounds such as sulfide and hydroxylamine, cysteamine is oxidized to the sulfinic acid derivative, hypotaurine. Most metabolic pathways, however, give hypotaurine as a precursor to taurine (the sulfonic acid). Scheme I encompasses nearly all possible reactions of cysteamine in the physiological environment.

Cysteamine and its major metabolite, hypotaurine, are known to be excellent scavengers of HOCl and other reactive oxygen species (ROS) and are more likely to act as antioxidants in vivo than taurine (3, 11, 12). These ROS can cause damage to DNA, proteins, and lipids in addition to causing radical damage and oxidative stress in animal cells (11, 13, 14). In addition to protection against radical damage in DNA, cysteamine can also act as a repair agent for DNA through the formation of the protective $RSSR^{\bullet -}$, which then reacts with the $DNA^{\bullet +}$ radical ion to regenerate DNA and form cystamine, the cysteamine disulfide (2, 3). The ability of cystamine to reversibly form disulfide links with the sulfhydryl groups at or near the active sites of enzymes is also important in regulation of several essential metabolic pathways (15, 16).

Our research group embarked on a series of studies to elucidate the kinetics and mechanisms of the oxidation of cysteamine and its S-oxides. Previous studies done in our laboratory on the cysteamine sulfinic acid, hypotaurine, have shown that it reacts quite rapidly with chlorite to give a mixture of taurine, monocloro- and dichloro-taurine (17). Oxidation is believed to occur simultaneously at the sulfur center (to give the sulfonic acid) and at the nitrogen center (to give the chloramines). The oxidation of taurine by chlorite (18) and bromate (19) showed that oxidation occurs only on the nitrogen centre to give the corresponding N-derivatives. The reaction was exceedingly slow, even with the most powerful oxidizing agents such as acidic bromate. The formation of *N*-bromo- and *N*-chloro-taurines is suggested as a possible mechanism by which taurine can moderate the oxidative toxicity of halogens and hypobromous and hypochlorous acid in the slightly basic physiological environments (20).

A recent study from our laboratory on the oxidation of cysteamine by iodine and acidic iodate showed that these mild oxidants only oxidized cysteamine to its dimer, cystamine (21). In this study, stronger oxidants bromine and acidic bromate have been used. The aim of the study reported in this manuscript was to investigate whether these oxidants also produced cystamine as a viable product or whether the oxidation proceeded to hypotaurine or all the way to taurine as well as the *N*-bromotaurines. Bromate is a precursor to HOBr, a particularly damaging oxidizing species in the physiological environment. Stimulated granulocytes produce oxidizing agents (especially H_2O_2) and secrete granular proteins into the extracellular medium, which contributes to their antimicrobial, cytotoxic, and cytolytic activities (22). Each group of cells contains a specific peroxidase, which catalyzes the reactions of hydrogen peroxide with halogens. The enzyme, myeloperoxidase, which is abundant in neutrophils, catalyzes the oxidation of Br^- ions by H_2O_2 to yield HOBr as a reactive and oxidatively damaging product (23).

Scheme I.

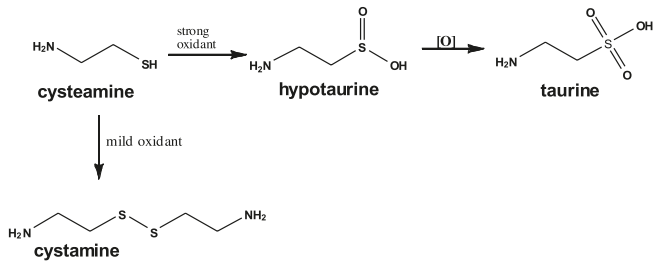

[R1] $H_2O_2 + Br^- + \text{Myeloperoxidase}/H^+ \rightarrow HOBr + H_2O$

Taurine and its precursors, e.g., hypotaurine and cysteamine have been suggested as possible moderators of HOBr toxicity by forming longer-lived and less oxidizing products in their reactions with HOBr (24).

Experimental

Materials

Cysteamine hydrochloride (CA, 2-aminoethanethiol hydrochloride) 98%, cystamine, bromine, potassium iodide, potassium bromide (Sigma-Aldrich), sodium perchlorate (98%) (Acros), sodium bromate, perchloric acid (72%), soluble starch, sodium thiosulfate, and hydrochloric acid (Fisher) were used without further purification. The concentration of bromine was determined by standardization against thiosulfate solution after addition of excess acidic iodide. Spectrophotometry was used as a complementary technique by measuring bromine absorbance at 390 nm where the extinction coefficient had been deduced to be 142 mol^{-1} L cm^{-1}. This standardization was carried out before each series of kinetic experiments owing to the volatile nature of bromine. CA solutions were prepared just before use and not kept for more than 24 h. All solutions were prepared using distilled and deionized water from a Barnstead Sybron Corporation water-purification unit. Inductively coupled plasma mass spectrometry (ICPMS) analysis showed negligible concentrations of iron, copper, and silver and approximately 1.5 ppb of cadmium and 0.43 ppb in lead as the most abundant metal ions, which was not enough to affect the overall reaction kinetics and mechanism (25).

Methods

All experiments were carried out at 25.0 ± 0.1 °C and a constant ionic strength of 1.0 mol/L ($NaClO_4$). CA, sodium perchlorate, and perchloric acid solutions were mixed in one vessel and bromate (or bromine) solutions in another. A PerkinElmer Lambda 25 UV–vis spectrophotometer interfaced to a Pentium IV computer was used for most of the kinetics and stoichiometric determinations. The slower BrO_3^- – CA reactions were monitored on the UV–vis spectrophotometer by monitoring bromine absorbance at 390 nm. Faster reactions were followed on a Hi-Tech Scientific SF61 – DX2 double mixing stopped-flow spectrophotometer.

Results

Stoichiometry

The stoichiometry of the BrO_3^- – cysteamine reaction in acidic medium is very complex. The reaction showed simultaneous oxidations at both the nitrogen and sulfur centers to give N-derivatives of the cysteamine sulfonic acid. Unlike what had been observed with other small organic sulfur molecules subjected to strong oxidizing agents, there is no cleavage of the C–S bond as evidenced by the lack of sulfate production. The reaction gives a mixture of products: $H_2NCH_2CH_2SO_3H$, $Br(H)NCH_2CH_2SO_3H$, and $Br_2NCH_2CH_2SO_3H$, all of which give nearly identical ^1H NMR spectra in the strongly acidic medium necessary for bromate oxidations.

Iodometric titrations in excess bromate conditions gave a reproducible stoichiometry consistent with a $6e^-$ oxidation of the sulfur center to the sulfonic acid, taurine, according to the following stoichiometric ratio:

$$[R2] \quad BrO_3^- + H_2NCH_2CH_2SH \rightarrow H_2NCH_2CH_2SO_3H + Br^-$$

In this titrimetric method, excess acidic bromate was reacted with a fixed amount of cysteamine and the excess oxidizing power left after complete consumption of cysteamine determined by addition of excess acidified iodide followed by a thiosulfate titration. Figure 1*a* shows a plot of thiosulfate titer vs. initial bromate concentrations. The plot is linear, as expected, with the intercept on the bromate concentration axis (zero thiosulfate titer) representing the exact amount of bromate needed to oxidize cysteamine. Data shown in Fig. 1*a* were taken with cysteamine fixed at 0.0020 mol/L. The intercept concentration on the bromate axis is 0.0021 mol/L, which is very close, within statistical error, to the 1:1 stoichiometric ratio of reaction [R2]. The UV spectrum of the product solution, on the other hand, shows a strong absorption peak at 244 nm, which is consistent with the formation of dibromotaurine. This is even more evident when Br^- is deliberately added to the reaction mixture to produce predominantly the dibromotaurine after prolonged standing.

$$[R3] \quad 5BrO_3^- + 3H_2NCH_2CH_2SH + Br^- + 6H^+ \rightarrow 3Br_2NCH_2CH_2SO_3H + 6H_2O$$

Reaction [R3] is preceded by the formation of monobromotaurine:

$$[R4] \quad 4BrO_3^- + 3H_2NCH_2CH_2SH + 3H^+ \rightarrow 3(Br)HNCH_2CH_2SO_3H + Br^- + 3H_2O$$

Direct reaction of cysteamine with aqueous bromine showed a clean 1:5 stoichiometric ratio:

$$[R5] \quad 5Br_2 + H_2NCH_2CH_2SH + 3H_2O \rightarrow Br_2NCH_2CH_2SO_3H + 8Br^- + 8H^+$$

Stoichiometry [R5] was deduced by mixing excess bromine solutions with a fixed amount of cysteamine and measuring the residual absorbance of bromine at 390 nm. None of the mono- or di-bromotaurine products absorb at 390 nm, and so all contribution to the absorbance at this wavelength was attributed solely to bromine. Figure 1*b* shows the data derived from such a series of experiments for a fixed concentration of 3.0×10^{-4} mol/L cysteamine. The intercept concentration of the $[Br_2]_0$ axis is 1.5×10^{-3} mol/L, which represents the exact amount of bromine needed to consume 3×10^{-4} mol/L cysteamine, which confirms the 1:5 stoichiometry.

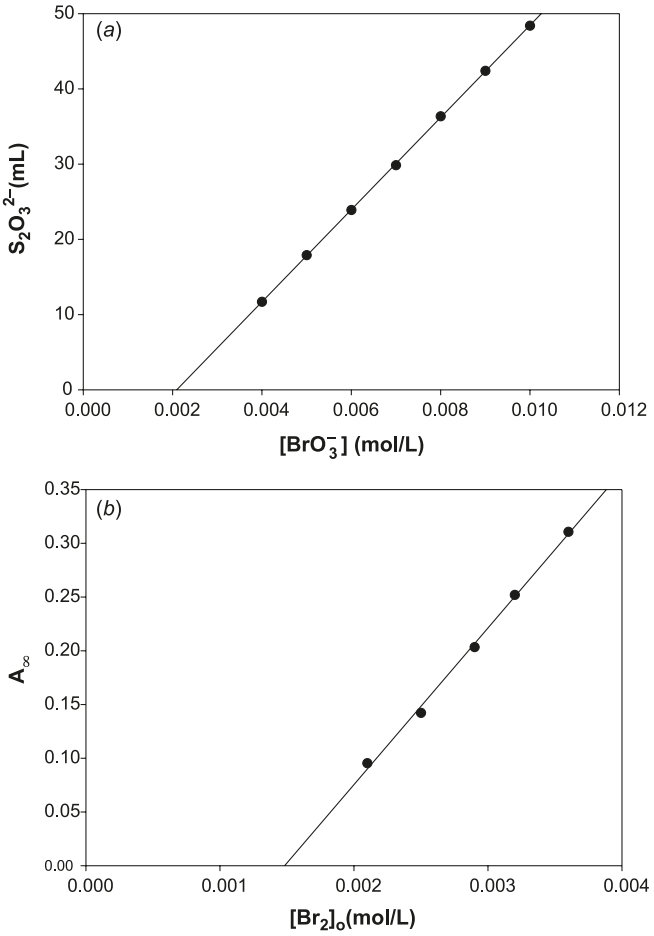

Fig. 1. (*a*) Iodometry titration for stoichiometry analysis of product solutions for a constant $[CA]_o$ and $[H^+]_o$ of 0.002 mol/L and 0.2 mol/L, respectively. $[BrO_3^-]$ = (a) 0.004 mol/L, (b) 0.005 mol/L, (c) 0.006 mol/L, (d) 0.007 mol/L, (e) 0.008 mol/L, (f) 0.009 mol/L, (g) 0.010 mol/L. This intercept represents the maximum amount of bromate tolerated by the reaction system before permanent bromine production is observed. (*b*) Plot of absorbance at infinity (A_∞) vs. $[Br_2]_o$ from the bromine oxidation of cysteamine. The intercept, as expected, is consistent with the stoichiometry equation proposed for the direct Br_2 – CA reaction. [CA] = 0.0003 mol/L, $[Br_2]_{intercept}$ = 0.0015 mol/L.

Monobromotaurine and dibromotaurine can be quantified in the reaction product by their rapid reaction with excess iodide to produce iodine, which could be determined spectrophotometrically and (or) titrimetrically:

$$[R6] \quad (Br)HNCH_2CH_2SO_3H + 2I^- + H^+ \rightarrow H_2NCH_2CH_2SO_3H + I_2\ (aq) + Br^-$$

Reaction [R6] is the reason why iodometric titrations in excess bromate only showed the formation of the sulfonic acid taurine (stoichiometry [R2]), and not the *N*-bromo derivatives. Their formation was masked, since they rapidly oxidized the iodide to iodine.

Product identification

Dibromotaurine was identified by its distinct UV spectrum featuring a sharp strong peak at 244 nm and a weaker peak at 336 nm (26). In addition to a peak also at 336 nm, monobromotaurine has an absorption peak at 288 nm (27) with a weak absorptivity coefficient of only 425 mol^{-1} L cm^{-1}. Bromine oxidations of cysteamine always produced mixtures of the mono- and di-bromotaurines, with the monobromotaurine's peak at 336 nm completely obscured by the contribution from dibromotaurine. Highly acidic environments favored monobromotaurine over dibromotaurine, since the ratio of the absorbance at 288:244 increased with a decrease in pH. This ratio also increased if taurine was added to the stoichiometric solution [R5]. Quantitative formation of monobromotaurine could be achieved by mixing an exact 1:4 ratio of cysteamine to bromine:

$$[R7] \quad 4Br_2 + H_2NCH_2CH_2SH + 3H_2O \rightarrow BrHNCH_2CH_2SO_3H + 7Br^- + 7H^+$$

^{1}H NMR spectra were also used to prove that the cysteamine carbon skeleton of two sets of methylene protons is not disturbed during its oxidation. Figure 2 shows the series of spectra representing the reactants and products. Spectrum A is of pure cysteamine in neutral pH showing the methylene proton triplets centered at 2.78 and 3.15 ppm. Spectrum B is of the product of cysteamine–bromate reaction in acidic medium. The two methylene triplets appear at 3.4 and 4.08 ppm with a larger coupling constant than observed with pure cysteamine. Spectrum C is of pure hypotaurine, while D is of the oxidation product of hypotaurine with acidic bromate. Spectrum E is the standard spectrum of taurine in D_2O at nearly neutral pH. The appearance of the methylene peaks upfield compared with the other spectra is due to the comparatively higher pH conditions utilized in the acquisition of this spectrum. Spectrum F is the product of the taurine–bromate reaction. Spectra B, D, and F are identical, showing that cysteamine, hypotaurine, and taurine are all oxidized by acidic bromate to the same final product. The two smaller triplets appearing on the bromate–taurine spectrum are due to the fact that this reaction produces a mixture of products, which also include the oxime, $H(OH)NCH_2CH_2SO_3H$ (28).

Reaction kinetics

As with all bromate oxidations, this reaction is only viable in highly acidic environments. The reaction could be monitored by following the appearance of bromine in excess bromate conditions. In this configuration, the reaction initially showed a quiescent period with no formation of bromine. We shall call this period the "induction period". The end of the induction period is signaled by the formation of bromine. Figure 3*a* shows a series of typical bromine absorbance traces derived from varying the initial bromate concentrations. At the end of the induction period, there is a

Fig. 2. ^{1}H NMR spectrum showing (A) cysteamine, (B) cysteamine + BrO_3^- + H^+, (C) hypotaurine, (D) hypotaurine + BrO_3^- + H^+, (E) taurine, and (F) taurine + BrO_3^- + H^+.

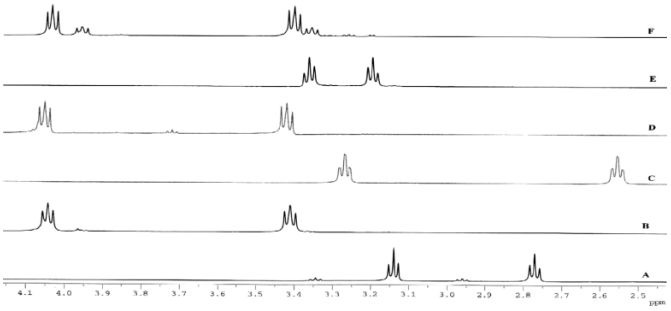

Fig. 3. (*a*) Effect of varying bromate concentration on the oxidation of CA by bromate. There is an increase in the rate of bromine formation as the bromate concentration is increased. $[CA]_o$ = 0.005 mol/L, $[H^+]_o$ = 0.2 mol/L, $[BrO_3^-]$ = (a) 0.05 mol/L, (b) 0.06 mol/L, (c) 0.07 mol/L, (d) 0.08 mol/L, (e) 0.09 mol/L, (f) 0.10 mol/L, (g) 0.11 mol/L. (*b*) Linear plot of reciprocal induction time vs. $[BrO_3^-]$ for data shown in Fig. 3*a*.

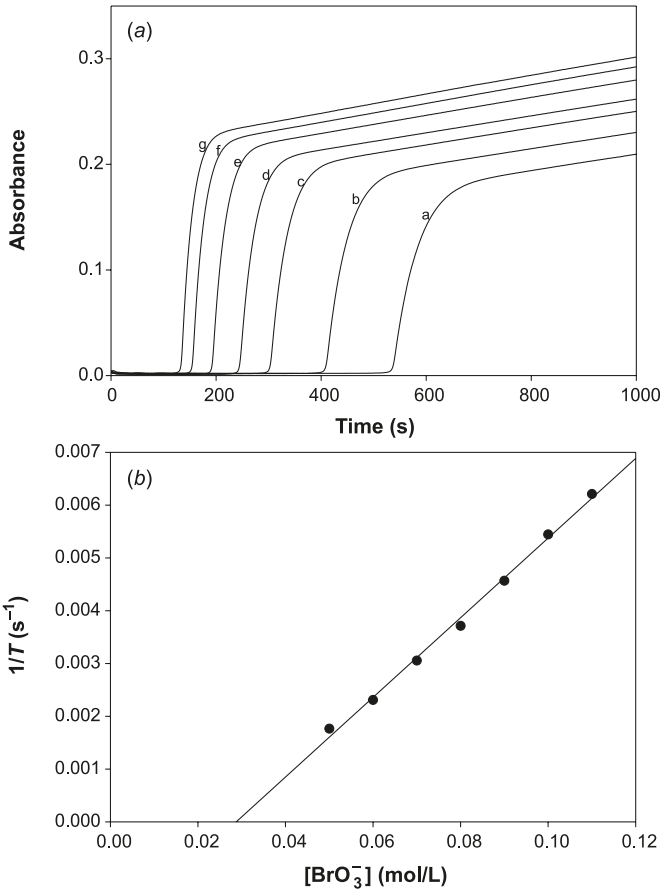

rapid formation of bromine, which eventually gives way to a slower rate of formation until the excess bromate or bromide formed from the reaction mixture has been exhausted, thus shutting down the BrO_3^-/Br^- reaction:

[R8] $BrO_3^- + 5Br^- + 6H^+ \rightarrow 3Br_2 + 3H_2O$

Figure 3*b* shows that the length of this induction period has an inverse linear dependence upon initial bromate concentrations. This would suggest that the precursor reaction to the formation of bromine depends on bromate concentrations to the first power. Figure 4*a* shows the reaction's dependence on acid concentrations, with Fig. 4*b* showing that the induction period follows an inverse squared dependence on acid that tends towards saturation as acid concentrations are further increased. The biphasic bromine formation in Fig. 4*a* is worth noting. Though higher acid concentrations reduce the induction period, they also reduce the amount of bromine formed in the rapid first step. The rate of formation of bromine in the slower phase appeared insensitive to variations in acid concentrations, and they also appear to be zero-order. Figure 5 shows that for as long as $[BrO_3^-]_0 \gg [CA]_0$, then the induction period will be invariant, but the rate and amount of bromine formed after the induction period varies with initial cysteamine concentrations. This trend would be expected, since reaction [R8] is catalyzed by bromide, and higher CA concentrations would produce higher bromide concentrations.

The direct reaction of bromine with CA was so rapid that its rate approached the detection limit of our stopped-flow apparatus. The only way to slow the reaction down so that it could be observed on our stopped-flow ensemble was to flood the reaction with bromide so that the reaction being observed was between CA and tribromide (see Fig. 6) (29, 30).

[R9] $Br_2 + Br^- \rightleftharpoons Br_3^-$; $K_{eq} = 17$

[R10] $3Br_3^- + H_2NCH_2CH_2SH + 3H_2O \rightarrow H_2NCH_2CH_2SO_3H + 6H^+ + 9Br^-$

The reaction involves a very fast initial step that is complete in less that 50 ms followed by a slower step that takes about 1.0 s. The initial step involves the consumption of approximately 3 equiv. of bromine to 1 equiv. of CA. This is equivalent to oxidizing CA to taurine:

[R11] $3Br_2 + H_2NCH_2CH_2SH + 3H_2O \rightarrow H_2NCH_2CH_2SO_3H + 6Br^- + 6H^+$

The formation of bromamines after formation of taurine appears to constitute the slower stage of the reaction. Figure 7 shows a series of experiments in which bromine is in excess of the stoichiometric amounts needed to satisfy reactions [R5] and [R7]. Trace a is a control experiment, which was not flooded with bromide. It shows that the reaction is complete within the mixing time of the stopped-flow instrument. The rest of the other traces show one single rapid step without a slower second step. No acid was added to this series of kinetics runs, and this appears to enhance the normally slower second step. The full 5:1 stoichiometry [R5] is attained within 0.5 s. Acid, however, was not inhibitory enough to allow for the determination of kinetics constants

Fig. 4. (*a*) Effect of progressively increasing $[H^+]$ at constant [CA] and $[BrO_3^-]$. $[CA]_o = 0.005$ mol/L, $[BrO_3^-]_o = 0.05$ mol/L, $[H^+]$ = (a) 0.20 mol/L, (b) 0.25 mol/L, (c) 0.30 mol/L, (d) 0.35 mol/L, (e) 0.40 mol/L, (f) 0.45 mol/L, (g) 0.50 mol/L, (h) 0.60 mol/L. (*b*) Plot showing the linear dependence of induction time on the reciprocal of $[H^+]_o^2$ for data shown in Fig 4*a*.

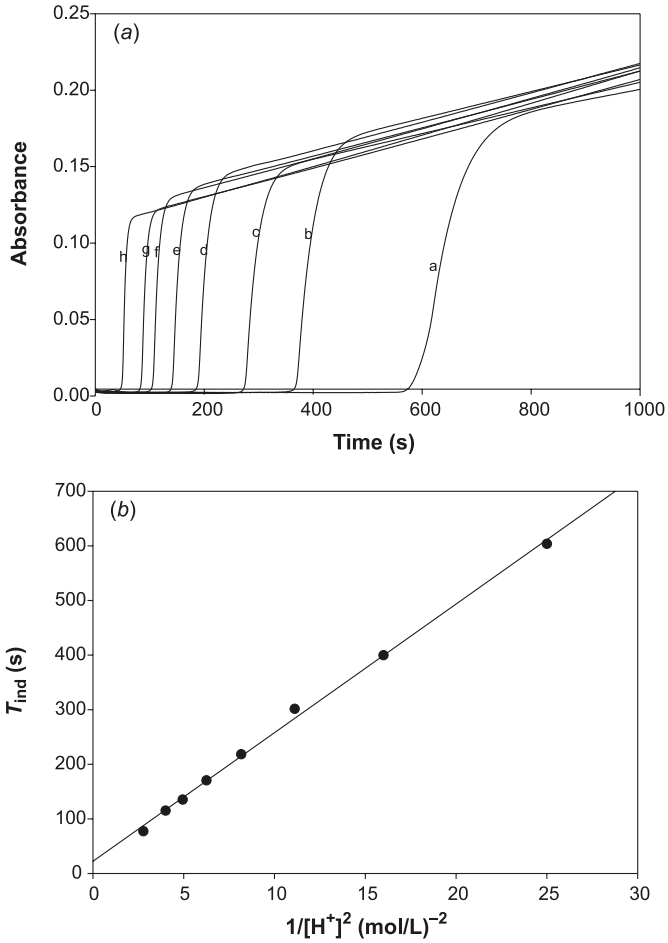

for the Br_2 – CA reaction, but it appeared to stunt the second slower part of the reaction in which bromamines are formed (see Fig. 8).

Mechanism

The rapid Br_2 – CA reaction implies that in both Figs. 1*a* and 3*a*, formation of bromine indicates complete consumption of CA. Any bromine formed in the presence of CA will be rapidly consumed and will not accumulate. The bromine–hypotaurine reaction was also found to be as rapid as the Br_2 – CA reaction; which implies that reaction [R2] has to run its course before bromine production commences.

The inverse bromate dependence and inverse square acid dependence of the induction period implies that the rate-determining step to reaction [R11] is the well-known standard bromate initiation reaction:

[R12] $BrO_3^- + 2H^+ + Br^- \rightleftharpoons HBrO_2 + HOBr$

We base our assertion on the following logic. The direct reaction of bromine and cysteamine (Figs. 6–8) is so rapid (close to diffusion-controlled) and much faster than the reac-

Fig. 5. "Peacock-tail type" traces obtained from variation of $[CA]_o$ in excess $[BrO_3^-]_o$ conditions. The final Br_2(aq) increases with $[CA]_o$, but the induction period does not change. $[BrO_3^-]$ = 0.1 mol/L, $[H^+]$ = 0.2 mol/L, [CA] = (a) 0.005 mol/L, (b) 0.006 mol/L, (c) 0.007 mol/L, (d) 0.008 mol/L, (e) 0.009 mol/L, (f) 0.010 mol/L, (g) 0.011 mol/L.

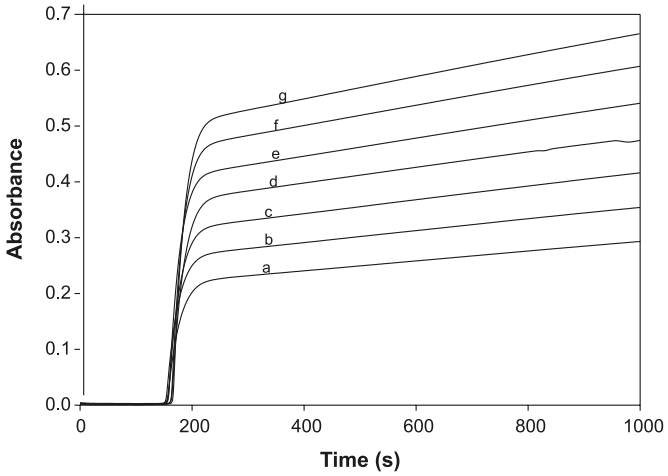

Fig. 6. Effect of varying CA on the direct reaction of Br_2 vs. CA in excess bromide monitored at 390 nm. $[Br_2]$ = 0.00215 mol/L, $[Br^-]$ = 1.0 mol/L, [CA] = (a) 0.0001 mol/L (b) 0.0002 mol/L (c) 0.0003 mol/L (d) 0.0004 mol/L (e) 0.0005 mol/L (f) 0.0007 mol/L.

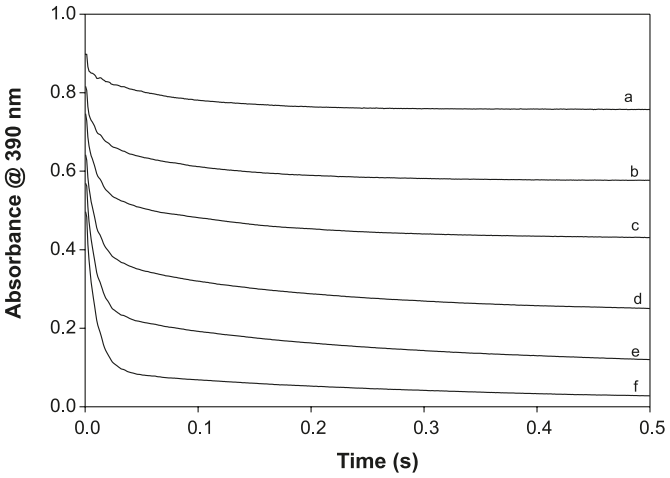

Fig. 7. Effect of varying $[Br_2]_o$ on the direct reaction of Br_2 vs. CA in excess bromide monitored at 390 nm. [CA] = 0.0003 mol/L, $[Br^-]$ = 1.0 mol/L, $[Br_2]$ = (a) 0.001 68 mol/L (no bromide), (b) 0.001 68 mol/L, (c) 0.002 10 mol/L, (d) 0.002 50 mol/L, (e) 0.002 93 mol/L, (f) 0.003 35 mol/L.

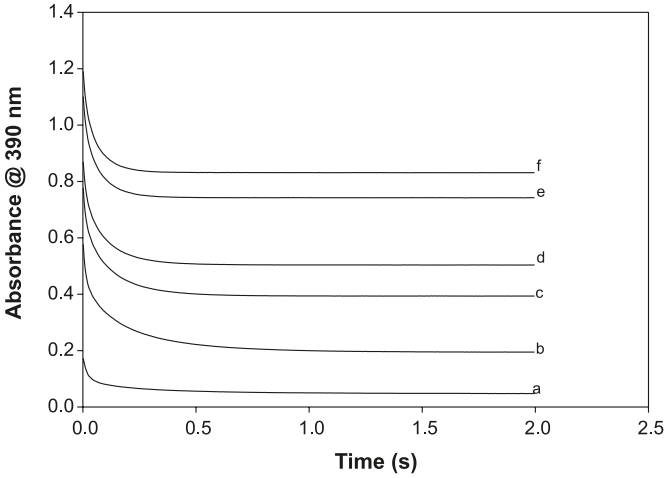

Fig. 8. Effect of acid on the bromine–CA reaction. Acid is mildly inhibitory on the first initial rapid phase of the reaction but shuts down the second slower section of the reaction, which involves formation of bromamines. $[Br_2]_o$ = 0.002 45 mol/L, $[CA]_o$ = 0.0004 mol/L, $[H^+]$ = (a) no acid, (b) 0.006, (c) 0.008, (d) 0.010, (e) 0.012, (f) 0.014 mol/L.

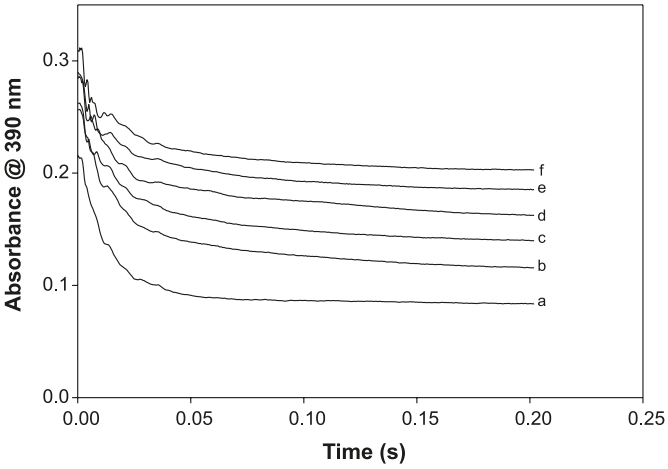

tion of bromate and cysteamine such that formation of bromine should indicate complete consumption of cysteamine. The time taken to achieve complete consumption of cysteamine (the induction period monitored in Figs. 3*b* and 4*b*), is inversely proportional to the rate of reaction (i.e., consumption of cysteamine).

Further reaction can occur between the reactive species $HBrO_2$ and HOBr with CA and its oxidative by-products.

[R13] $HOBr + H_2NCH_2CH_2SH \rightarrow H_2NCH_2CH_2SOH + Br^- + H^+$

While $HBrO_2$ can also act as oxidizing agent as in reaction [R13], its rapid disproportionation in the presence of bromide (reaction [R14]) will make its effect as an oxidant negligible.

[R14] $HBrO_2 + Br^- + H^+ \rightleftharpoons 2HOBr$

If one re-writes reaction [R13] and substitutes CA with any 2-electron reductant (i.e., the 2 electrons can be supplied by any oxidizable species in the reaction mixture), then a linear combination of R12 + 3R13 + R14 gives an overall reaction stoichiometry that is autocatalytic in Br^-:

[R15] $BrO_3^- + 6H^+ + Br^- + 6e^- \rightarrow 2Br^- + 3H_2O$

As long as reaction [R12] is the rate-determining step, Br^- will be an autocatalyst. All bromate solutions contain trace amounts of bromide in the reaction mixture, which have

Table 1.

No.	Reaction	k_f, k_r
M1	$BrO_3^- + 2H^+ + Br^- \rightleftharpoons HBrO_2 + HOBr$	2.1, 1.00×10^{-4}
M2	$HBrO_2 + Br^- + H^+ \rightleftharpoons 2HOBr$	2.00×10^6, 2.00×10^{-5}
M3	$HOBr + Br^- + H^+ \rightleftharpoons Br_2 + H_2O$	8.9×10^9, 1.10×10^2
M4	$2HBrO_2 \rightleftharpoons BrO_3^- + HOBr + H^+$	4.00×10^7, 2.00×10^{-10}
M5	$Br_2 + Br^- \rightleftharpoons Br_3^-$	1.50×10^9, 8.8×10^7
M6	$BrO_3^- + H^+ \rightleftharpoons HBrO_3$	1.00×10^7, 1.00×10^9
M7	$H^+ + HBrO_3 \rightleftharpoons H_2BrO_3^+$	1.00×10^6, 5.0×10^8
M8	$H_2BrO_3^+ + H_2NRSH \rightarrow HBrO_2 + H_2NRSOH + H^+$	6.45
M9	$HBrO_2 + H_2NRSH \rightarrow HOBr + H_2NRSOH$	5.00×10^3
M10	$HOBr + H_2NRSH \rightarrow H^+ + Br^- + H_2NRSOH$	5.00×10^6
M11	$HOBr + H_2NRSOH \rightarrow H^+ + Br^- + H_2NRSO_2H$	5.00×10^5
M12	$HOBr + H_2NRSO_2H \rightarrow H^+ + Br^- + H_2NRSO_3H$	1.00×10^3
M13	$Br_2 + H_2NRSH + H_2O \rightarrow 2H^+ + 2Br^- + H_2NRSOH$	5.00×10^8
M14	$Br_2 + H_2NRSOH + H_2O \rightarrow 2H^+ + 2Br^- + H_2NRSO_2H$	2.50×10^8
M15	$Br_2 + H_2NRSO_2H + H_2O \rightarrow 2H^+ + 2Br^- + H_2NRSO_3H$	1.70×10^3
M16	$Br_2 + H_2NRSO_3H \rightarrow BrHNRSO_3H + H^+ + Br^-$	3.30
M17	$Br_2 + BrHNRSO_3H \rightleftharpoons Br_2HNRSO_3H + H^+ + Br$	7.00×10^{-2}, 1.05×10^{-3}
M18	$2BrHNRSO_3H + H^+ \rightleftharpoons Br_2HNRSO_3H + H_2NRSO_3H$	5.00, 1.00×10^{-2}

Note: The units for the kinetics constants in the third column are derived from the reaction's molecularity except where water is involved, in which case water was ignored.

been measured at approximately 5.0×10^{-6} mol/L. Quantitatively, are these sufficient to initiate the reaction? A computer simulation of the reaction while utilizing these trace bromide concentrations gave much slower reaction kinetics and longer induction periods when compared with the experimental traces. This suggests that there should be another pathway that generates bromide ions, which will initiate reaction [R12]. Another pathway that exists for initial bromide formation involves oxidation by protonated bromic acid (31–33):

[R16] $H^+ + BrO_3^- \rightleftharpoons HBrO_3$

[R17] $H^+ + HBrO_3 \rightleftharpoons H_2BrO_3^+$

[R18] $H_2BrO_3^+ + H_2NCH_2CH_2SH \rightarrow H_2NCH_2CH_2SOH + HBrO_2 + H^+$

[R19] $HBrO_2 + H_2NCH_2CH_2SH \rightarrow H_2NCH_2CH_2SOH + HOBr$

Bromide ions will thus be generated by the successive reduction of bromate to bromide. Adding the sequence R16 + R17 + R18 + R19 + R13 and assuming each reductant can be represented by 2 e's; the overall reaction representing initial bromide formation will be similar to [R15] without the autocatalysis:

[R20] $BrO_3^- + 6H^+ + 6e^- \rightarrow Br^- + 3H_2O$

The autocatalytic route will take over and become dominant as the reaction proceeds and rate of bromide production shifts from the kinetics derived from [R20] to those derived from [R15]. As bromide ions accumulate, their rate of production ceases to be the rate-determining step, and reaction [R12] takes over as the overall rate-determining step. Data shown in Figs. 3*b* and 4*b* strongly suggests that reaction [R12] is rate-determining up to the stage where cysteamine is completely converted to taurine.

All kinetics data collected imply that the oxidation of CA to taurine is much faster than the subsequent N-bromination reactions. Since bromate oxidations are only viable at low pH conditions, in all bromate oxidations of CA studied, the CA should be fully protonated on the amino group:

[R21] $H_2NCH_2CH_2SH + H^+ \rightleftharpoons HSCH_2CH_2NH_3^+$; K_b

The protonation of the amino group should retard the electrophilic bromination of this group:

[R22] $HSCH_2CH_2NH_3^+ + Br_2 \rightleftharpoons HSCH_2CH_2NHBr + Br^- + 2H^+$

An intermediate such as $HSCH_2CH_2NHBr$ should be very unstable and should rapidly hydrolyze to the sulfenic acid, since the thiol group is much more easily oxidizable than the N-containing group:

[R23] $HSCH_2CH_2NHBr + H_2O \rightarrow H_2NCH_2CH_2SOH + Br^- + H^+$

N-bromination of the sulfenic acid and hypotaurine will also be insignificant owing to kinetics factors in which the oxidation of the sulfur group is much more rapid than N-bromination (see Table 1).

N-bromination kinetics

In neutral to slightly basic environments, reaction [R24] should be very rapid and almost diffusion-controlled.

[R24] $HO_3SCH_2CH_2NH_2 + Br_2 \rightarrow HO_3SCH_2CH_2NHBr + Br^- + H^+$

Our stopped-flow ensemble, with a mixing time of 3 ms, could not catch this step, nor the next step that involves formation of the dibromo derivative:

[R25] $HO_3SCH_2CH_2NHBr + Br_2 \rightleftharpoons HO_3SCH_2CH_2NBr_2 + Br^- + H^+$

This reaction is slower in highly acidic medium because reactions of type [R22] are slower than those of type [R24]. Electrophilic attack on the N-center by bromine is retarded by the protonation of the nitrogen center. Kinetics data in Figs. 6 and 7 show first-order kinetics in both bromine and cysteamine. If one was to assume, in a limiting case, that the route of bromination through [R22] is negligible, then the initial rate of N-bromination would be given by the equation,

$$[1] \qquad \text{Rate} = -\frac{d[Br_2]}{dt} = \frac{k_{24}[HO_3SCH_2CH_2NH_2]_T[Br_2]_0}{1 + K_b[H^+]}$$

$[HO_3SCH_2CH_2NH_2]_T$ is the total cysteamine sulfonic acid concentration before it is partitioned into the protonated and unprotonated forms. Retardation by bromide ions can be mathematically handled in the same manner, in which rate of reaction becomes

$$[2] \qquad -\frac{d[Br_2]}{dt} = \frac{k_{24}[HO_3SCH_2CH_2NH_2]_T[Br_2]_0}{\{1 + K_b[H^+]\}\{1 + K_{eq}[Br^-]\}}$$

In none of our experiments were the retardations by Br^- and H^+ effective enough for the use of eqs. [1] and [2] in determining bimolecular rate constant k_{24}. We could only use initial rate data and assuming bimolecular kinetics in Fig. 8 to estimate that k_{24} should be larger than 10^5 mol^{-1} L s^{-1}. Reliable values for k_{24} can be derived from relaxation techniques (34). In the physiological environment and in basic conditions, in general, the major route of N-bromination (reaction [R26]) is through hypobromous acid (35), since the bromine hydrolysis reaction favors hypobromous acid at high pH and aqueous bromine in acidic conditions (36).

[R26] $HO_3SCH_2CH_2NH_2 + HOBr \rightarrow HO_3SCH_2CH_2NHBr + H_2O$

N-bromination in bromate oxidations is predominantly through aqueous bromine, since bromate oxidations only proceed in acidic environments (37).

The acid retardation observed for the reaction shown in Fig. 8 may suggest that reaction [R26] is slower than [R24]. Previous studies have confirmed that the monobromo-and dibromo- derivatives are affected by acid, with highly acidic conditions favoring monobromotaurine (37). This means that while [R24] can proceed quantitatively to the product monobromotaurine, [R25] is an equilibrium condition in which high acid concentrations in the products can swing the equilibrium towards monobromotaurine formation. The addition of taurine to dibromotaurine solutions saw the decrease in the peak at 244 nm (dibromotaurine) and the emergence of a peak at 288 nm (monobromotaurine):

[R27] $HO_3SCH_2CH_2NH_2 + HO_3SCH_2CH_2NBr_2 \rightleftharpoons 2HO_3SCH_2CH_2NHBr$

Scheme II.

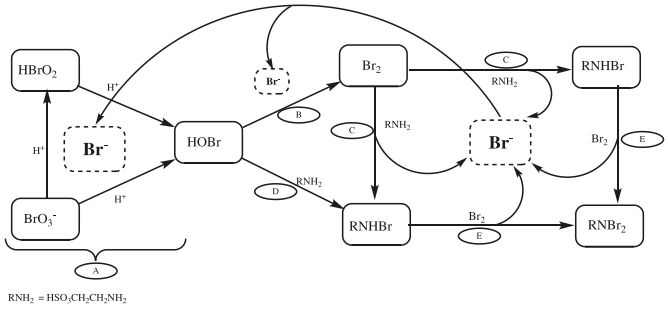

Bromine formation

There is only one reaction in the reaction mixture responsible for bromine formation:

[R28] $HOBr + Br^- + H^+ \rightleftharpoons Br_2(aq) + H_2O$

Since both HOBr and Br_2 react rapidly with cysteamine (and its metabolite, hypotaurine), then formation of bromine is an indicator that cysteamine and its metabolites have all been oxidized to at least the taurine stage. The formation of bromine at the end of the induction period should depend in some manner on the rate of formation of bromide (assuming excess of acidic bromate). The full reaction network responsible for bromine formation is complex, and can be depicted by the network shown in Scheme II. To simplify this scheme, only the relevant reactions after cysteamine has been oxidized to taurine (presented as RNH_2 in the scheme) are included. It is a bromide-controlled network due to bromide's role as an autocatalyst in the reaction network. It provides a positive feedback loop that feeds into reaction A and accelerates the reaction.

This network scheme can explain the rate of bromine formation after the induction period as well as the biphasic nature of bromine production. Without excess bromate the feedback loop cannot exist, since reaction [R12] is a precursor to all autocatalysis. The reaction network relies on process B being fast (reaction [R28]). Our simulations also showed that HOBr does not accumulate to concentrations higher than 10^{-6} mol/L for the duration of the reaction. The fact that process C is faster than E delivers the biphasic bromine formation. Since bromine formation depends on bromide formation, the faster N-bromination of taurine ensures a fast rate of formation of bromide and subsequently a high rate of initial formation of bromine. Higher acid concentrations retard the formation of dibromotaurine. Figure 4*a* illustrates this effect: high acid concentrations catalyze the formation of HOBr, leading to higher bromine formation (processes A + B). This in turn leads to higher bromide formation (process C), which feeds back into process A. Acid catalysis of A is stronger than acid retardation of C. However, acid retardation of E is significant and when most of the monobromotaurine has been formed, the subsequent bromination to dibromotaurine is slower (in high acid), and the equilibrium of reaction [R25] is shifted to the left. With process E slower, bromide formation is slower, and subsequently bromine formation is slow, as observed in the slower bromine formation in the second phase. The zero-order kinetics observed in bromine formation is due to the fact that this section is no longer solely dependent on

Fig. 9. Simulated results (symbols) of traces *a* and *c* (solid lines) from Fig. 3*a* showing the effect of bromate variation on CA oxidation.

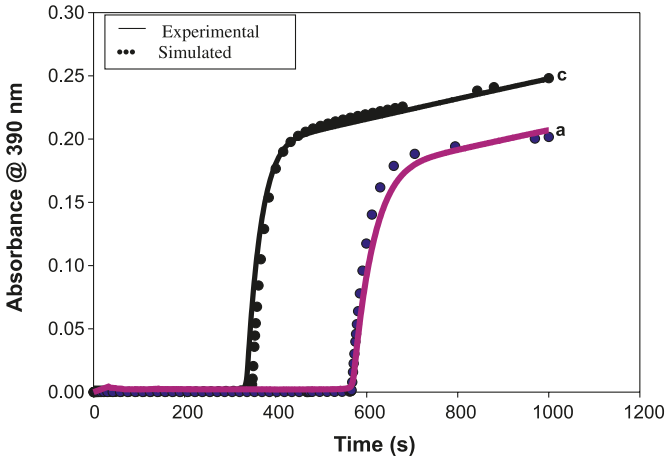

process A, but a much more complex network. Primarily, equilibrium [R25] acts as a valve in the release of bromide and maintains a constant release of bromide ions, as in drug-suspension reactions.

Overall reaction mechanism and simulations

The overall mechanism that can explain the observed global dynamics of the system on the basis of Scheme II is shown in Table 1. The first group of reactions M1–M4 and M5 are the well-known oxybromine reactions whose kinetics constants are well known (31, 33, 39–41). These were not varied during the simulations and were accepted as "fixed". The next set of reactions M6–M10 constitute the initiation reactions whose sole purpose is to produce bromide ions (autocatalytically). Protolytic reactions such as M6 and M7 are normally diffusion-controlled. The use of diffusion-controlled rate constants for these reactions rendered the simulations too stiff, necessitating hours of computer time instead of mere seconds with the use of the kinetics constants used in Table 1. The adopted kinetics constants did not deliver any different simulation results when compared to the use of the diffusion-controlled kinetics constants. The third set of reactions M11–M15 constitute the oxidation of cysteamine to taurine. The major oxidants are HOBr and Br_2. Even though this set of reactions is fast, they are all controlled (after the initiation reactions), by reaction [R12] (M1 in the table). Rapid reaction [R28] (M3 in table) is also controlled by [R12], since production of Br^- is a prerequisite reagent for formation of HOBr. The N-bromination reactions are listed in the last section, M16–M18. We have assumed in all these simulations that we are dealing with a protonated taurine molecule on the amino group, since the pH conditions necessary for the activity of bromate as an oxidant are low enough to protonate that group. Since we did not and could not quantify the degree of acid retardation by the reaction, we felt that this was a reasonable assumption. Reaction M18 was a necessary disproportionation reaction in high-acid conditions. Even in low-acid conditions, reaction M18 ensured that stoichiometry [R7] was attained first before stoichiometry [R5]. The simplicity of the simulations was derived from the bottle-neck offered by reaction M1, irrespective of the other reaction rates. The initiation reactions were important in establishing the time taken before bromine formation commenced, but a few seconds into the reaction reactions M6–M10 ceased to be effective. Since we could not harness the bromination reactions due to their speed, the lower-limit-estimated rate constants were effective, since ultimately, formation of bromine was controlled by M1. Figure 9 shows a reasonably good fit to the data on bromate-dependence data shown in Fig. 3*a*. A good fit was also obtained with acid-dependence traces shown in Fig. 4*a*. The model was able to satisfactorily predict both bromate- and acid-dependence effects with respect to induction period and rate of formation of bromine at the end of this induction period.

Conclusion

The reversible nature of N-bromination of the taurine formed after a full oxidation of cysteamine suggests that cysteamine and its oxidation metabolites are capable of moderating hypobromous acid and hypochlorous acid toxicities by forming these long-lived brominated derivatives. The ease of regeneration of taurine in reducing conditions means that this moderation can proceed indefinitely in a cyclic manner.

Acknowledgement

This work was supported by research grant no. CHE 0614924 from the National Science Foundation.

References

1. Z.M. Bacq. Int. J. Sulfur Chem. B, **6**, 94 (1971).
2. L.D. Buckberry and P.H. Teesdale-Spittle. Sulfur–hydrogen compounds. *In* Biological interactions of sulfur compounds. *Edited by* S. Mitchell. London. 1996. p. 113.
3. P. Wardman. Thiol reactivity towards drugs and radicals: Some implications in the radiotherapy and chemotherapy of cancer. *In* Sulfur-centered reactive intermediates in chemistry and biology. *Edited by* C. Chatgilialoglu and K.D. Asmus. New York. 1990. p. 415.
4. R.J. Cremlyn. An introduction to organosulfur chemistry. John Wiley & Sons, Chichester. 1996.
5. J. Darkwa, R. Olojo, E. Chikwana, and R.H. Simoyi. J. Phys. Chem. A, **108**, 5576 (2004).
6. S.V. Makarov, C. Mundoma, J.H. Penn, J.L. Petersen, S.A. Svarovsky, and R.H. Simoyi. Inorg. Chim. Acta, **286**, 149 (1999).
7. S.V. Makarov, C. Mundoma, J.H. Penn, S.A. Svarovsky, and R.H. Simoyi. J. Phys. Chem. A, **102**, 6786 (1998).
8. A.G. Renwick. Sulfur-containing drugs and related compounds– Chemistry, biology, and toxicology. Ellis Horwood, Chichester, NY. 1987.
9. A.G. Renwick. Sulfur–oxygen compounds. *In* Biological interactions of sulfur compounds. *Edited by* S. Mitchell. London. 1996. p. 42.
10. A.E. Miller, J.J. Bischoff, and K. Pae. Chem. Res. Toxicol. **1**, 169 (1988).
11. O. Aruoma, B. Halliwell, B. Hoey, and J. Butler. Biochem. J. **256**, 251 (1988).
12. D. Becker, S. Summerfield, S. Gillich, and M.D. Sevilla. Int. J. Radiat. Biol. **65**, 537 (1994).

13. A. Del Corso, P.G. Vilardo, M. Cappiello, I. Cecconi, M. Dal Monte, D. Barsacchi, and U. Mura. Arch. Biochem. Biophys. **397**, 392 (2002).
14. M. Hermes-Lima and T. Zenteno-Savin. Comp. Biochem. Physiol. Part C: Toxicol. Pharmacol. **133**, 537 (2002).
15. F. Martin, M.F. Penet, F. Malergue, H. Lepidi, A. Dessein, F. Galland, M. de Reggi, P. Naquet, and B. Gharib. J. Clin. Invest. **113**, 591 (2004).
16. N.B. McDonnell, R.N. DeGuzman, W.G. Rice, J.A. Turpin, and M.F. Summers. J. Med. Chem. **40**, 1969 (1997).
17. B.S. Martincigh, C. Mundoma, and R.H. Simoji. J. Phys. Chem. A, **102**, 9838 (1998).
18. C.R. Chinake and R.H. Simoyi. J. Phys. Chem. B, **101**, 1207 (1997).
19. R.H. Simoyi, K. Streete, C. Mundoma, and R. Olojo. South African J. Chem. (Suid-Afrikaanse Tydskrif Vir Chemie), **55**, 136 (2002).
20. S.T. Test, M.B. Lampert, P.J. Ossana, J.G. Thoene, and S.J. Weiss. J. Clin. Invest. **74**, 1341 (1984).
21. A. Chanakira, E. Chikwana, D. Peyton, and R. Simoyi. Can. J. Chem. **84**, 49 (2006).
22. E.L. Thomas, M.B. Grisham, and M.M. Jefferson. J. Clin. Invest. **72**, 441 (1983).
23. E.L. Thomas, P.M. Bozeman, M.M. Jefferson, and C.C. King. J. Biol. Chem. **270**, 2906 (1995).
24. A.J. Jesaitis and E.A. Dratz. Molecular basis of oxidative damage by leukocytes. CRC Press, Fla. 1992.
25. J. Darkwa, R. Olojo, E. Chikwana, and R.H. Simoyi. J. Phys. Chem. A, **108**, 5576 (2004).
26. R.H. Simoyi, K. Streete, C. Mundoma, and R. Olojo. South African J. Chem. (Suid-Afrikaanse Tydskrif Vir Chemie), **55**, 136 (2002).
27. E.L. Thomas, M.B. Grisham, D.F. Melton, and M.M. Jefferson. J. Biol. Chem. **260**, 3321 (1985).
28. R.H. Simoyi, K. Streete, C. Mundoma, and R. Olojo. South African J. Chem. (Suid-Afrikaanse Tydskrif Vir Chemie) **55**, 136 (2002).
29. M.-F. Ruasse, J. Aubard, B. Galland, and A. Adenir. J. Phys. Chem. **90**, 4382 (1986).
30. Z. Toth and L. Fabian. Inorg. Chem. **43**, 2717 (2004).
31. C.E. Sortes and R.B. Faria. J. Braz. Chem. Soc. **12**, 775 (2001).
32. R.D. Faria, I.R. Epstein, and K. Kustin. J. Phys. Chem. **98**, 1363 (1994).
33. Gy. Rabai, Gy. Bazsa, and T.M. Beck. Int. J. Chem. Kinet. **13**, 1277 (1981).
34. D.H. Turner, G.W. Flynn, N. Sutin, and J.V. Beitz. J. Am. Chem. Soc. **94**, 1554 (1972).
35. E.L. Thomas, P.M. Bozeman, M.M. Jefferson, and C.C. King. J. Biol. Chem. **270**, 2906 (1995).
36. R.C. Beckwith, T.X. Wang, and D.W. Margerum. Inorg. Chem. **35**, 995 (1996).
37. R.H. Simoyi, K. Streete, C. Mundoma, and R. Olojo. South African J. Chem. (Suid-Afrikaanse Tydskrif Vir Chemie), **55**, 136 (2002).
38. R.M. Noyes, R.J. Field, and R.C. Thompson. J. Am. Chem. Soc. **93**, 7315 (1971).
39. R.M. Noyes. J. Am. Chem. Soc. **102**, 4644 (1980).
40. I. Szalai, J. Oslonovitch, and H.D. Forsterling. J. Phys. Chem. A, **104**, 1495 (2000).